University of Michigan, Honors Thesis

Effect of Nanofiber Size and Alignment of Electrospun Scaffolds on Neuronal Differentiation

By: Annie Yingyao Song

Concentration: Cell & Molecular Biology and Biomedical Engineering (CMB:BME)

Table of Contents

Abstract

Fiber size and orientation, along with other topographical features, are important aspects in developing nanofibrous scaffolds for neural tissue engineering. In this study, poly(lactic acid) (PLLA) scaffolds composed of random and aligned fibers were fabricated with electrospinning technique. The diameters of the electrospun fibers were varied by adjusting the PLLA concentration in solution. Mouse embryonic stem cells (ESC) were cultured on the different scaffolds. Gene expression analysis and cell morphology studies were carried out to assess neuronal differentiation of the seeded ESC. The cells exhibited significantly different degrees of differentiation depending on the size and orientation of the fibers. Based on the experimental results, the aligned fibers better promoted neuronal differentiation than the random fibers. For random fibers, those with an average diameter of 700 nm were optimal. And for aligned fibers, those around 1.3 μm induced the most expression of neurite cytoskeleton protein, and thus, best promoted neuronal differentiation.

Introduction

Many diseases damage the body in ways that are beyond repair, meaning treatments are only effective at alleviating the symptoms of diseases. Using regenerative medicine, researchers are creating methods that can actually replace defective tissues and organs to restore normal functions. An emerging research area, regenerative medicine has the potential to revolutionize treatments for diseases such as degenerative joint conditions, neurological disorders, wounds and injuries, as well as diabetes and heart disease. It will also combat the problems of transplant rejection and donor shortage for millions of patients in need of organ transplants.

Tissue engineering is an innovative approach for regenerative medicine that focuses on using biomaterial scaffolds to support tissue regeneration. This field combines the efforts of engineering, biology and material science to tackle some of the most significant clinical issues. Although much of tissue engineering currently stays at the experimental stage, it proves to have tremendous clinical potential [1][2][3]. The subfield of neural tissue engineering is driven by the goal of creating effective treatments for nerve repair. Nervous tissue is one of the four basic tissue types in our body. The nervous systems have crucial roles in coordinating our sensations and movements, as well as maintaining the proper functioning of internal organs. Moreover, unlike the other cells, most neurons lack the ability to regenerate in their native environment. Therefore, recovery is extremely difficult for patients with damaged nervous tissues, as a result of spinal cord injuries and other disease. The World Health Organization estimated in 2006 that neurological disorders affect as many as one billion people worldwide [4]. Thus, neural regeneration is an important task for tissue engineering.

Tissues are made of cells and the extracellular matrix (ECM) they secrete and organize. Cell-ECM interaction has direct control over cell behaviors [5]. The biomaterial scaffolds mimic natural ECM structures to create a microenvironment, allowing cells to adhere, proliferate and differentiate into desired lineages [6]. In another word, the scaffold is a 3D substrate for cells and should finally be replaced by the cell-produced ECM. Thus, there are several key characteristics that the scaffolds should have in order to be successful [7]. First, they need to be

highly porous to allow cell infiltration and diffusion of both nutrients and wastes. Second, they should have fitting mechanical properties depending on the type of tissue in question. For example, the scaffold for soft tissue regeneration is a lot more compliant than that for bone. Third, the scaffold materials must be biocompatible and biodegradable, which means that they can avoid inciting human immune response and safely break down inside the body. A variety of natural materials, like collagen, fibrin and chitosan, as well as synthetic polymers, such as poly(lactic acid) (PLLA), poly(glycolic acid) PGA, poly(caprolactone) PCL and co-polymers, can be used to construct nanofibrous scaffolds for tissue regeneration. In this study, PLLA is used, which already has FDA approval for applications such as surgical sutures [8].

The basic philosophy behind the biomimetic scaffolds is to mimic functions of collagen, the main ECM protein for every major tissue. Collagen protein has triple-helix structure (i.e. tropocollagen), which generally consists of two identical peptide chains and an additional chain that differs slightly in its chemical composition. There are several types of collagen, in which the most abundant type in human is Type I collagen. After being secreted into the extracellular space, multiple tropocollagen molecules form collagen fibrils, via covalent cross-linking by enzyme lysyl oxidase. Multiple collagen fibrils group together into collagen fibers of around 50-500 nm (i.e. nanofibers) [9][10]. Thus, the biomaterial scaffolds described above are also referred to as “nanofibrous scaffolds”. One question might arise is that why not only use natural collagen to fabricate the scaffolds for tissue engineering purposes. The answer is that the use of collagen as a scaffolding material has challenges, which include: pathogen transmissions, less control over mechanical property and degradability, as well as the overall batch-to-batch inconsistency of materials derived from biological sources [11]. Thus, current nanofibrous scaffolds are fabricated with different materials, depending on the specific applications.

There are currently three major methods to make biomaterial scaffolds: self-assembly [12], electrospinning [13] and phase separation [14]; each has its own advantages and disadvantages [7]. Electrospinning is a well-established technique to fabricate scaffolds, and the most commonly used method in nerve tissue regeneration. It was shown that electrospun scaffolds

are feasible as platform for ESC propagation and neuronal differentiation [15]. The disadvantages of electrospinning include: difficulty fabricating 3D shapes, little control over porosity or pore shape, beading in fibers that are low in diameters [7]. The process is briefly described as following: polymer is dissolved in solvent and loaded onto a syringe pump; upon applying high voltage, the solution is ejected as a stream, the solvent evaporates and the polymers undergo thinning and elongation to form nanofibers, which deposit on a collector plate to create the scaffold films. Choosing an optimal solvent is important for constructing electrospun scaffolds. A wider diameter distribution was shown with PLLA in 70:30 Dichloromethane: Dimethylformamide (DCM:DMF) than in Hexafluoroisopropanol (HFIP) [16]. The reason is that HFIP is more polar and acts as a better hydrogen bond donor, so PLLA is more stable in HFIP [17].

To fabricate scaffolds with different fiber sizes, the concentration of PLLA polymer in solution is varied, and the higher the PLLA concentration, the larger the fiber diameter [18]. The orientation of nanofibers in a scaffold can either be random or aligned. To collect random fibers, a flat, vertical collector plate is used. To collect aligned fibers, a cylinder is used as the collector plate that rotates at a very high rate, which exerts a tangential force on the polymer to line up the resultant fibers [18].

Nanofibers in the electrospun scaffolds have physical and chemical characteristics that can influence how biological molecules will be adsorbed, and thus regulate cell adhesion. In neural tissue engineering, scaffold fibers can provide many focal adhesion points for cell attachments and therefore help orient neurite (i.e. dendrites and axons) growth, which is referred to as contact guidance. It was found that aligned fibers provide better contact guidance for neural stem cell differentiation than random fibers [18][19][20]. It was also shown that aligned electrospun PCL nanofibers promoted differentiation of ESC into neurons by directing neurite extension over significant distance [21]. However, it is not always obvious how fiber size affects neural differentiation. In a previous study, differentiation of neural stem cells was higher on PLLA fibers of around 300 nm than on those exceeding 1µm, independent of fiber arrangement [18]. Whereas, another study showed that 500 nm fibers are the most promising among the

different sized aligned fibers for promoting proliferation and neurite outgrowth of neural stem cells, and that 350 nm and 1.15 μm are the most promising for random fibers [19].

In order to successfully engineer viable tissues, cells need to be seeded on the scaffolds. Both primary and stem cells can be used. Primary cells are taken directly from native tissues and cultured. One challenge is that the cells in culture usually undergo phenotypic changes. Stem cells, on the other hand, are harder to harvest and culture at the beginning. However, they have more potential for proliferation and differentiation [22]. Numerous types of adult stem cells (e.g. mesenchymal stem cells, adipose tissue-derived stem cells, neural stem cells, hematopoietic stem cells) as well as ESC have been used. Over the past few decades, intense studies have led to much progress in elucidating stem cell renewal and differentiation mechanisms. ESC are pluripotent cells that have the potential of continuous self-renewal. ESC also hold great therapeutic promises for treatments of diseases. Its clinical potential is especially studied for nerve repair for both central and peripheral nervous systems. After injecting neural progenitors derived from ESC into rats with injured spinal cords, it was shown that there was modest functional recovery [23]. Another group explored the potential of motor neurons derived from ESC to restore functional motor units (skeletal muscle fibers and innervating neuron) [24]. It was also shown that ESC-derived neural progenitor cells promoted repair of transected sciatic nerve [25][26]. In vivo studies like those mentioned above involving ESC therapy had limited success because the injected cells were not always properly localized and oriented. Thus, finding the optimal biomaterial scaffolds as a means of structuring and organizing ESC is an important research focus. The combination of ESC therapy and scaffolds will be a better strategy for nerve repair. The hope is that scaffolds can help control cell fate, and ultimately reproduce nervous tissues of clinically relevant size, so they can bring about functional recovery in patients.

In the present study, PLLA and electrospinning technique are used to fabricate nanofibrous scaffolds that can potentially promote differentiation of mouse ESC into neuronal cells. More specifically, the focus is to study two key parameters of the biomaterial scaffolds that may affect neuronal differentiation: one is nanofiber size, and the other is nanofiber orientation.

Neuronal differentiation involves activation of multiple genes, and the level of transcription of TUBB 3 is the basis for gene expression analysis in this study. Also, immunofluorescence study was employed for the detection of TUBB 3's encoded product - Class III β-tubulin (i.e. β3-tubulin). This protein is composed of 450 amino acids, with molecular weight of 50,433 Da. The tubulin proteins are globular proteins that are divided into 5 families, one of which is β-tubulins that heterodimerize with α-tubulins to form microtubules, an important cytoskeleton component. In particular, β3-tubulin is primarily expressed in neurons, and it is part of the microtubules that make up neurites. This protein is involved in guiding neurite growth and maintenance, and it has a critical role in neurogenesis. Comparing gene and protein levels for cells cultured on different scaffolds is a crucial evaluation of the scaffolds' potential in enhancing neuronal differentiation. This study is meaningful in that it contributes to finding the optimal scaffold for neural tissue engineering, which is the essential first step of forming viable, high-ordered nervous tissues that can ultimately be used in human disease treatment.

Material and Methods

1. Scaffold Fabrication

Poly(L-lactide) (PLLA) with an inherent viscosity of approximately 1.6 dL/g was purchased from Boehringer Ingelheim (Ingelheim, Germany). Solvent HFIP was purchased from Sigma-Aldrich, USA.

All the PLLA scaffolds, with aligned or random fibers, were fabricated by electrospinning technique. Polymer solution was prepared by dissolving PLLA into HFIP for 6%, 8% and 15% PLLA concentration (W/V) (%). The polymer solution was fed into a 10mL plastic syringe fitted with an 18 G needle with a diameter of 1.2 mm. An applied voltage of 15 kV was provided by a DC power supply (160 Series, Warner Electric, Michigan) and a feeding rate of 1.5mL/h were used, which is controlled by a syringe pump (14831200, Fisher Scientific, USA). The linear rate of the rotating disk at the edge was set to 2000 rpm. The distance between the needle tip and the collectors was 15cm. A flat aluminum collector was used to fabricate random fibers while a rotating disk was used for aligned fibers. The resulting PLLA fibers were collected on the 22 x 22 mm coverslips placed at the respective collectors and used for cell culture study.

2. Structural characterization of PLLA Scaffold

The scaffolds were coated with gold using a sputter coater (SPI Module Sputter Coater, USA). The morphologies of the scaffolds were then studied via scanning electron microscopy (SEM) (Philips XL30FEG, FEI Company, USA) with an accelerating voltage of 15 kV. With an image analysis software (Image J, National Institutes of Health, USA), data of fiber diameter can be obtained using SEM images.

3. Cell Culture and Seeding

ES-D3 mouse embryonic stem cells were obtained from the Sue O'Shea lab (University of Michigan) and cultured in 25cm^2 canted neck culture flasks (Corning, USA) coated with a 0.1% gelatin solution and 10 μg/mL leukemia inhibitory factor (LIF1005, EMD Millipore, Massachusetts, USA). Cells were cultured in Dulbecco's Modified Eagle Medium (DMEM) (Sigma,

USA) supplemented with 10% fetal bovine serum (FBS) (Gibco, Life Technologies, USA), 10^{-4} M β-mercaptoethanol (Sigma, USA), 0.022% mM L-glutamine (Sigma-Aldrich, USA), and 0.13% 4-(2-hydroxyethyl)-1-piperazineethanesulfonic acid (HEPES) (Sigma-Aldrich, USA). The cells are passaged every two days at a ratio of 1:4.

After reaching about 70% confluence, the cells were detached by 0.25% Trypsin (Gibco, Life Technologies, USA). PLLA scaffolds were sterilized using UV light for 1 hour. Then the cells were seeded onto PLLA scaffolds, placed in 6-well plates with the density of 2×10^4 cells/cm^2. The control groups were cultured with regular media described aboved (i.e. non-directional media), and the treatment groups were cultured in neuro-permissive media, which contains 20% Neurobasal media (Gibco) and 80% F-12 Nutrient Mixture (Gibco), containing 0.4% B27 (Gibco) and 0.8% N2 supplement (Gibco).

4. Gene Expression Analysis

RNA Isolation

Cells seeded on scaffolds were harvested after 1 week and 2 weeks. There were 12 samples each – 6 cultured in regular media, 6 cultured in neuro-permissive media. Total RNA was prepared as described in the RNeasy Mini Kit (Qiagen, Valencia, CA, USA), which also enriches for mRNA.

Reverse Transcriptase PCR

Next, the RNA was turned into more stable cDNA by Reverse Transcriptase PCR. About 1 µg total RNA from each sample was used for Oligo(dT)20 – primed reverse transcription, which was carried out as described in the product protocol of TaqMan reverse transcription reagents (Applied Biosystems, Foster City, CA, USA)

Real Time PCR

Quantitative PCR reactions were carried out with TaqMan Universal PCR Master Mix (Applied Biosystems) and specific primers for Gapdh (pre-designed, TaqMan Gene Expression Assay, ID Mm99999915_g1) and Tubb3 collagen type II (pre-designed, TaqMan Gene Expression Assay, ID

Mm00727586_s1). Signals were detected with a ViiA 7 Real Time PCR System (Applied Biosystems). Glyceraldehyde-3-phosphate dehydrogenase (GAPDH) is a gene whose expression level does not differ among samples, so it was used as the endogenous reference gene. The expression of target gene TUBB 3, a direct indicator of neuronal differentiation, was compared with that of GAPDH, so that the target gene expression can be normalized to the amount of input cDNA. For each sample, 2 μL of cDNA was added as template in PCR reactions. Relative quantitation of gene expressions will be performed using the comparative C_T method (ABI Prism 7700 Sequence Detection System).

5. Cell Morphology and Neurite Outgrowth Studies - Confocal Fluorescence Microscopy

Immunofluorescent labeling was performed, using series of procedures, to observe and compare neurite outgrowth of differentiating ESC seeded onto different PLLA scaffolds.

Scaffolds with cells seeded were rinsed twice with phosphate buffered saline (PBS), fixed in 3.7% formaldehyde in PBS for 6 minutes at room temperature. Then, the constructs were washed with PBS and stored in 1mL PBS in 4^{o}C. Cell-scaffold constructs were then permeabilized with 0.2% Triton X-100 for 6 minutes at room temperature and washed with PBS 3 times. Non-specific labeling was blocked by incubating with goat serum (diluted, at 1:10 ratio, in 1% bovine serum albumin (BSA) in PBS) overnight in 4^{o}C.

Then the samples were incubated in primary antibody (β3-tubulin antibody (TUJ-1)), mouse monoclonal IgG (Santa Cruz Biotechnology, Santa Cruz, CA) at 1:500 dilutions overnight at room temperature. Samples were rinsed with PBS three times, then incubated with fluorescein isothiocyanate (FITC)-labeled secondary antibody (goat anti-mouse IgG, Santa Cruz Biotechnology) at 1:100 dilutions for 1 hour at room temperature in the dark. The antibodies were for labeling β3-tubulin so that neurites could be detected as distinct threadlike extensions (fluoresces green). The samples were washed three times, then taken out of the 6-well plates and transferred from the glass coverslips to slides. They were mounted using mounting medium containing 4'-6-diamidino-2-phenylindole (DAPI) to label DNA and thus mark the presence of all cells (blue). Coverslips (22 x 50 mm) were used to cover the samples on the slides, which were

observed under a confocal fluorescence microscope (Nikon C1 Upright Confocal Microscope).

6. Statistical Analysis

Diameter measurements

n = 60 for each sample. Measurements were taken using the SEM images for each scaffold to obtain the mean and standard deviation values. The 2-sided 2-sample t-tests were conducted to determine significant differences between pairs of diameter measurements. The significance level was $\alpha = 0.001$; thus, a results is significant if $p < 0.001$.

Gene Expression

n = 3 for each of the samples to obtain the mean and standard deviation values. The single sided 1-sample t-tests were conducted to determine significant differences between pairs of data. The ΔC_T values and ΔC_T standard deviation values were used for the t-tests (ABI Prism 7700 Sequence Detection System). The significance level was $\alpha = 0.05$; thus, a results is significant if $p < 0.05$.

Results

1. Characterization of Electrospun PLLA Scaffolds

PLLA fibers with different topographies were fabricated by optimizing the processing conditions of electrospinning. In this study, the PLLA fibers in each group were designated by a capital letter followed by a number; the letter indicates orientation of the fibers (i.e. R = random, A = aligned), the number indicates concentration of PLLA in solution used to make the fibers (i.e. 6 = 6%, 8 = 8% or 15 = 15%).

It was found that the fiber diameter increased as the concentration of the polymer solution increased (Fig. 1), which was consistent with previous reports [18][19]. The aligned PLLA fibers exhibited a high order of arrangement, independent of fiber diameter. The statistical distribution of fiber diameters was further determined for both the aligned and random PLLA fibers, as shown in Table 1.

The effect of different collector plate on diameter size was also investigated - stationary collector plate used to fabricate random fibers, versus rotating collector plate used to fabricate aligned fibers. There was no significant difference between fiber diameters of R6 and A6, and between R8 and A8. However, A15 fibers are found to be significantly thinner than R15 fibers.

All but R6 and A6 fibers had smooth uniform surfaces, independent of fiber arrangement (Fig 1). R6 and A6 fibers, which are made with the lowest concentration of PLLA, showed beading.

Table 1. Properties of Different PLLA Electrospun Fibers.

	R6	R8	R15*	A6	A8	A15*
Fiber Diameter	293 nm	702 nm	1.57 um	313 nm	682 nm	1.32 um
SD	62 nm	156 nm	179 nm	71 nm	169 nm	249 nm

The asterisks (*) indicate concentration of PLLA in solution that resulted in random and aligned fibers having significantly different diameters with $p < \alpha = 0.05$, using 2-sided 2-sample t test.

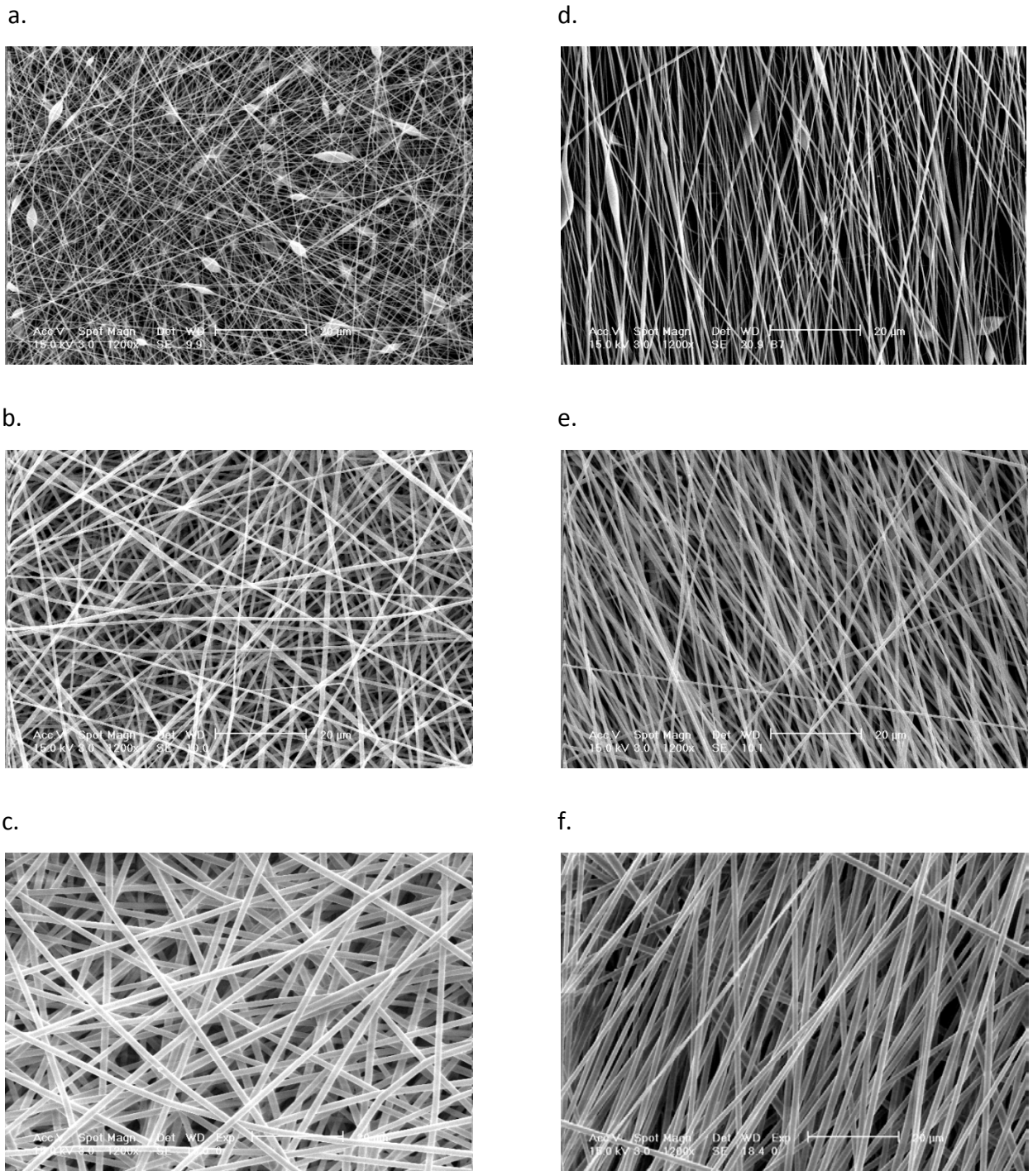

Figure 1. Scanning electron micrographs of PLLA electrospun fibers with different dimensions and patterns: a) R6, b) R8, c) R15, d) A6, e) A8, f) A15. The length of the reference bar is 20 µm.

2. Gene Expression Studies

The number of mouse ESC seeded on each of scaffolds with different topographies is theoretically the same. Thus, cells on each PLLA scaffold can be harvested and total expressions of gene TUBB 3 can be quantified using Real Time PCR, which directly indicates the level of ESC differentiation and allows for comparisons. Fig. 2 shows the expressions of target gene after 1 week and 2 weeks of culturing on PLLA scaffolds. It is important to note that using the comparative C_T method for Real Time PCR, the relative expression value for ND-R6 in each set of data is defined to be 1, and the other values in the set are calculated relative to it. This also means that values from different data sets are not directly comparable.

As shown in Fig. 2a and 2c, TUBB 3 was expressed in all samples in the study. The ESC cultured in neuro-permissive media expressed TUBB 3 at higher levels than control ESC cultured in non-directional media (Fig. 2b, d). The week 1 cells in non-directional media expressed low level of TUBB 3, relative to the week 1 cells in neruo-permissive media (Fig. 2a). Whereas, week 2 control groups in non-directional media displayed higher relative expressions of the gene (Fig. 2c).

In terms of trend in gene expression for different fiber sizes, week 1 cells on random fibers (cultured in neuro-permissive media) showed increasing gene expression as fiber size increased (Fig. 2b). Whereas, week 2 cells on random fibers (cultured in neuro-permissive media) showed a decreasing trend (Fig. 2d). Both week 1 and week 2 cells on aligned fibers (cultured in neuro-permissive media) show increasing gene expression as fiber size increased (Fig. 2b, d).

Comparing random fibers and aligned fibers, the average of relative TUBB 3 expressions for A6, A8 and A15 (about 0.953) is higher than the average for R6, R8 and R15 (about 0.839) for week 1. Similarly, the average of the relative expressions for A6, A8 and A15 (about 1.089) is higher than the average for R6, R8 and R15 (about 0.914) for week 2. However, more reliable tests could not be done because of the inconsistency in the trend in data for random fibers.

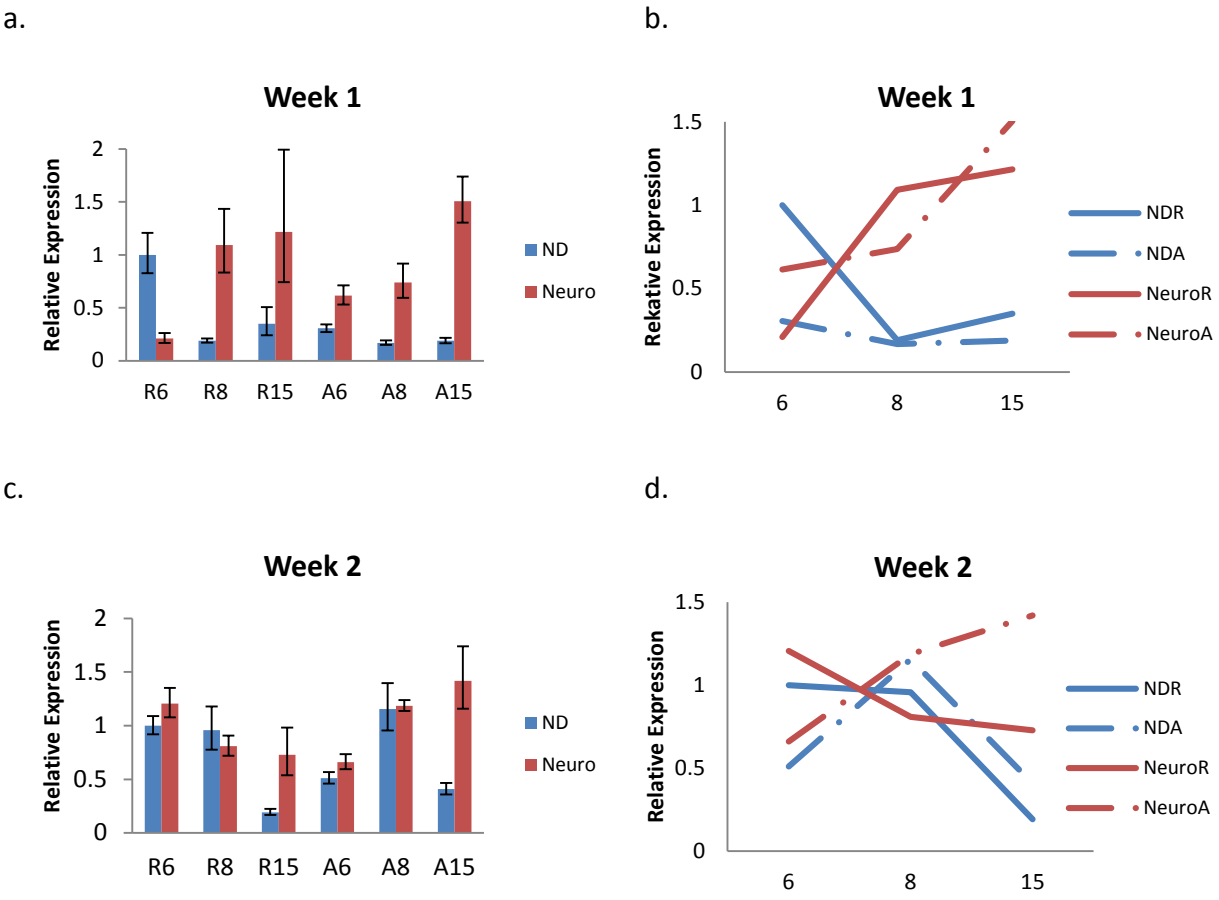

Figure 2. Relative expression of β3-tubulin by cells cultured on different PLLA scaffolds, in non-directional or neuro-permissive media after: a) b) 1 week, c) d) 2 weeks. "ND" - non-directional media, "Neuro" - neuro-permissive media.

Next, more in-depth analysis was done to investigate the trend in aligned nanofibrous scaffolds (i.e. A6, A8 and A15). Fig. 3 shows the increasing trend in TUBB 3 expression with significance testing. Besides the two partial sets of data presented above in Fig. 2 (Fig. 3a, b), two additional data sets for week 2 cells are also included (Fig. 3c, d). Fig 3a shows that the weeks 1 cells on A15 fibers expressed significantly more TUBB 3 than those on A6 fibers and A8 fibers. Fig. 3b shows that week 2 cells on A8 and A15 fibers expressed significantly more β3-tubulin than those on A6 fibers, respectively. Fig. 3c and 3d reinforce the findings in Fig 3b. Thus, A15 fibers were the best out of the three aligned fibers for promoting TUBB 3 expression.

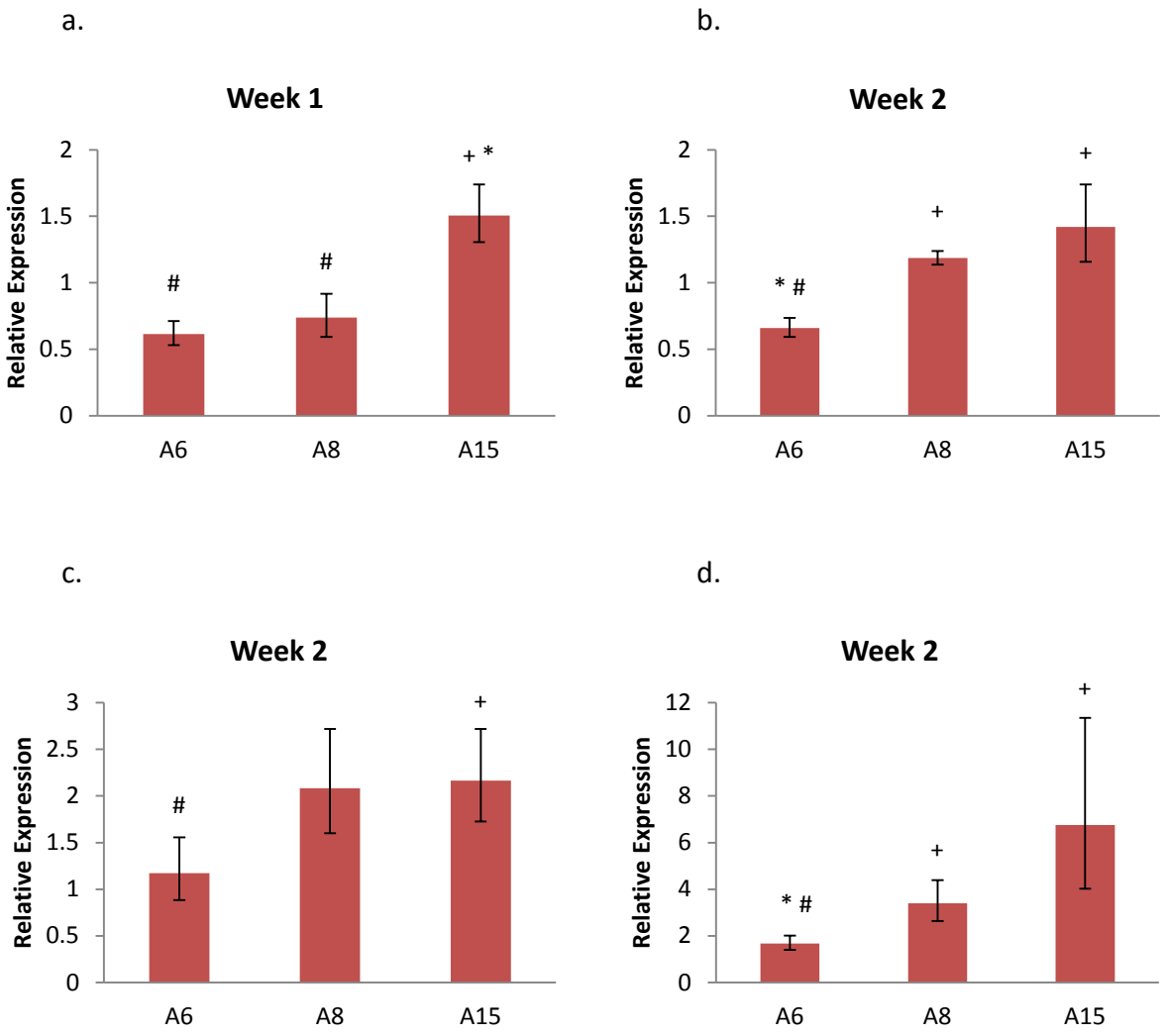

Figure 3. Relative expression of β3-tubulin by ESC cultured on aligned PLLA scaffolds, in neuro-permissive media after: a) 1 week, b) c) d) 2 weeks (3 independent samples). The symbols indicate significant differences with $p<0.05$, using 1-sided 2-sample t test: (+) - compared with A6, (*) -compared with A8, (#) - compared with A15.

3. Cell Morphology Studies

To observe the expression of β3-tubulin by ESC and the relationship between the protein and topographies of the scaffolds, immunocytochemistry staining and confocal microscopy observation were performed on cells at the end of 1 week. Fig. 4 represents the immunofluorescent micrographs of ESC on control and treatment samples on random and

aligned scaffolds with different diameters. Mouse anti-β3-tubulin conjugated to FITC fluoresced green, which marked the expression of protein β3-tubulin. Nuclei were stained blue by DAPI.

The cells in most samples formed large aggregates, except for cells on R15 fibers in neuro-permissive media. Overall, cells cultured in neuro-permissive media (Fig. 4g-l) express more β3-tubulin than corresponding control cells in non-directional media (Fig. 4a-f).

It was observed that cells seeded on aligned fibers expressed more target protein than those seeded on random fibers. For the control groups (ND), it was obvious that ESC seeded on A8 (Fig. 4e) and A15 (Fig. 4f) showed more β3-tubulin detection than ESC on R8 (Fig. 4b) and R15 (Fig. 4c), respectively. Similarly, for the treatment groups (NP), ESC seeded on A6, A8 and A15 (Fig. 4j-l) showed more β3-tubulin detection than ESC on R6, R8 and R15 (Fig. 4g-i), respectively. In addition, neurites (NP) extended out in random directions on R6 and R8 (Fig. 4g, h). However, neurites (NP) followed one general direction on each of the aligned scaffolds (Fig. 4j-l): in Fig. 4j and Fig. 4l, the neurite direction was close to vertical, slanted at a small angle; in Fig. 4k, the neurite direction was close to horizontal, slanted at a small angle. The nuclei on the aligned scaffolds (Fig. 4j-l) also seemed to be elongated along the axes of respective neurite direction; this was especially evident for sample A15 (Fig. 4l).

Based on samples in neuro-permissive media, within both random and aligned fibers, the amount of target protein expression and neurite outgrowth appeared to depend on the size of fibers. Out of the 3 random nanofibrous scaffolds (Fig. 4g-i), R8 promoted the most β3-tubulin expression. It was unexpected that there was scarce detection of β3-tubulin on R15 fibers (Fig. 4i). Out of the 3 aligned scaffolds (Fig. 4j-l), the neurite outgrowth was most extensive on A8 (Fig. 4k), and both neurites and nuclei were most aligned on A15 (Fig. 4l). Thus, R8 seemed to be the best random fiber size for enhancing neuronal differentiation, assuming R15 images were accurate. It could not be clearly concluded from the immunofluorescence images whether A8 or A15 had the best aligned fiber size in this study.

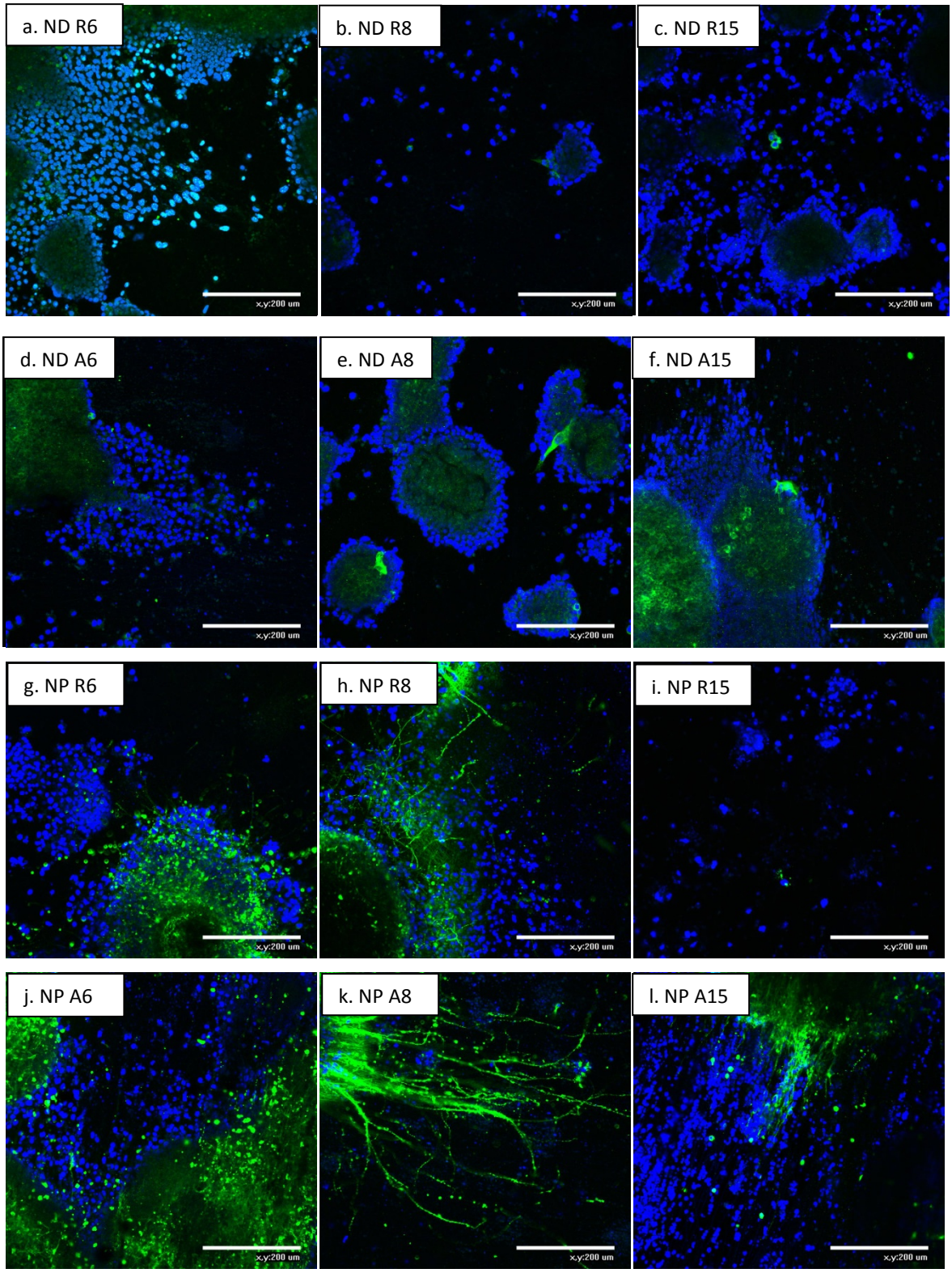

Figure 4. Immunostained β3-tubulin protein expressed by ESC on different scaffolds, cultured in non-directional media (ND): a) R6, b) R8, c) R15, d) A6, e) A8, f) A15; cultured in neuro-permissive media (NP): g) R6, h) R8, i) R15, j) A6, k) A8, l) A15. Green – mouse anti-β3-tubulin conjugated to FITC; Blue - DAPI. The length of the reference bar is 200 µm.

Discussion and Conclusion

Topographical features have been shown to influence important cell behaviors, such as adhesion, proliferation and differentiation [27][28][29]. Several works have been studying how electrospun nanofibrous scaffolds with different physical characteristics can affect cell fate, some of which focus on neural issue engineering. These studies examined the effect of fiber diameter of random fibers on neural stem cell differentiation [30], the differentiation into several different neural lineages of embryonic stem cells on aligned and random PCL nanofibers [21], and the potential for electrospun nanofibers to regulate neuron and astrocyte proliferation [31]. One area that still remains unclear is how fiber size and alignment of electrospun nanofibers can influence differentiation of ESC into neuronal cells.

In this study, nanofibrous scaffolds with different topographies were fabricated by adjusting the processing parameters. The fibers varied in diameter and arrangement. Replacing the stationary collector plate in electrospinning with a rapidly rotating collector plate caused the nanofibers to line up and form aligned nanofibrous scaffolds. It was also shown that the fiber diameter increased with increasing PLLA concentration in solution for both random and aligned fibers.

The size of larger fibers made with 15% PLLA solution depended on the fiber orientation; this dependence was absent for the fibers made with 6% and 8% PLLA solutions. The A15 fibers were thinner than the R15 fibers, despite that the PLLA concentration was the same. This can be explained by considering the electrospinning process. When the polymer jet flows from the ground plate to the rotating wheel collector, fibers are attracted to the wheel and wind themselves around the circumference in a parallel array. In the process, the collector exerts a pulling force on the jet and stretches the nanofibers, and thus, reduces the diameter [18][32]. In this study, this stretching effect was pronounced in the larger fiber, but not in the smaller ones. This could be due to the fact that the ambient humidity was high enough to accelerate the solidification of PLLA nanofibers in the polymer jet, which largely overrode the stretching effect. However, when PLLA concentration was high, solidification process was slower and stretching of the fibers became significant [33].

It was also observed that, when the concentration was low (6%), there was beading on scaffolds (Fig. 1a, d). This is due to the fact that high solubility of polymer in solvent results in beading in smaller fibers, as PLLA is relatively soluble in HFIP [17]. The thin fibers are more likely to break after being ejected, so the ends of the fibers coil up and form beads. It is possible that beading can have an effect on cell adherence and proliferation, but it has not been clearly documented.

All the groups of cells seeded on the scaffolds expressed some level of TUBB 3 (Real Time PCR results), as well as the protein product β3-tubulin (confocal microscopy results). It was remarkable that cells in non-directional media were also differentiating. This indicated that the ESC could differentiate towards the neuronal lineage in the presence of the nanofibers, even without the aid of neuronal-specific biochemical agents. One important reason that nanofibrous scaffolds promote differentiation is through enhancing cell adhesion and proliferation, which is achieved by their superior ability to adsorb serum proteins. Compared to solid walled scaffolds, a study showed that nanofibrous scaffolds enhances adsorption of serum proteins by 4.2 times, and that fibers selectively adsorbed more ECM proteins that contain integrin-binding sequence (i.e. RGD), such as fibronectin and vitronectin [35]. It was also shown that the nanofibrous scaffolds improved cell attachments by 1.7 times in fetal bovine serum. This is important because cell-ECM interactions participate directly in mediating important cellular processes, including proliferation and differentiation [5]. Cell adhesion, in particular, precedes cell spreading, differentiation and functioning. Considering that the nanofibrous scaffolds and the solid walled scaffolds were made of the same PLLA, had the same porosity and pore structures, the study proved that the nanofibrous architecture alone provided a more favorable environment for cell adhesion. This agrees with the finding of the present study that all ESC were differentiating into neuronal cells on the nanofibrous scaffolds, even for the ones that did not have neuronal-specific factors in the environment.

It was shown that the ESC cultured in neuro-permissive media supported differentiation more than the cells cultured in non-directional media. This agreed with what was anticipated because

the neural-permissive media contains factors like B27 and N2 that specifically induce neuronal differentiation [34].

Previous studies have provided a variety of conclusions in terms of how different fibers size in aligned fiber scaffolds affects differentiation. One study showed that the aligned fibers at 500 nm were the best at promoting differentiation in neural stem cells [19]. Another work showed the 300 nm aligned fibers were optimal [18]. In this present study, through gene expression analysis, it was observed that the A15 fibers with average diameter of 1.32 μm seemed to be the best aligned fibers at promoting ESC differentiation into neuronal lineage.

Immunofluorescence staining was done to observe the expression of β3-tubulin protein, a cytoskeletal protein in neurite. The results showed that for random fibers, fiber size of around 700 nm (R8) induced the most expression of β3-tubulin and the highest degree of neuronal differentiation. However, the lack of staining for R15 fibers remained questionable, and additional experiments are needed to confirm the results. For aligned fibers, the immunofluorescence images did not completely agree with the Real Time PCR results in that the A8 fibers seemed to promote more β3-tubulin expression and neurite outgrowth, and A15 fibers caused the cell nuclei and neuritis to be more aligned. Considering that there was substantial positive staining for the A15 fibers, and immunofluorescence experiment was not repeated, the conclusion about aligned fiber size drawn from multiple trials of Real Time PCR was not rejected.

The straight forward explanation for why larger fibers (both random and aligned) tend to supports neuronal differentiation better is that they provide more space for the stem cells to adhere to, which induce more cell proliferation and differentiation. There are also other important factors that need to be taken into consideration. It was shown that as the fiber diameter decreased, there was an increase in total fiber surface area, which led to increased adsorption of growth factors and cytokines from serum in the media [19]. The cells have receptors for these media factors, which caused them to attach to the fibers and allow for differentiation. However, another opposing factor is scaffold pore size. The large diameter

fibers resulted in larger pores and allow for better cell infiltration and oxygen and nutrient diffusions [36]. As a result, more cells would survive and proliferate, and thus are able to attach to the fibers and undergo neuronal differentiation in favorable conditions. Consequently, the optimal fiber size for this study is a result of the balance between surface area of the fibers and pore size produced by interwoven fibers in the scaffold.

For the effect of fiber arrangement, the results of Real Time PCR study suggested that aligned fibers were better at promoting neuronal differentiation than the random fibers. However, a lack of significance for the results and a discord in the trends for the data of random fibers did not allow solid conclusions.

On the other hand, analysis with immunofluorescence staining clearly showed that the aligned nanofibrous scaffolds were better at promoting neuronal differentiation than the respective random nanofibrous scaffolds. First, there were more β3-tubulin expression and neurite extension from cells seeded on the aligned fibers. Furthermore, the neurites and nuclei on each aligned scaffold were oriented in one main direction, which was most likely the orientation of the aligned PLLA fibers that the cells were attached to. Current literature on nanofiber alignment documented that ESC followed contact guidance by growing their neurites parallel to the PLLA fibers. The majority of differentiating ESC also exhibited bipolar shape and had the longer axis of their cell bodies aligned with the fiber orientation [18]. Contact guidance was proven to work through focal adhesions – proteins that appeared as filament-like structures, extended out from the stem cell bodies and neurites and attached to the aligned nanofibers [18]. In contrast, these structures were not observed between cells and the random fibers. This demonstrated the extensive cell-scaffold interactions exhibited by the aligned fibers, which are responsible for promoting neuronal differentiation and orienting the differentiating cells. In the present study, the contact guidance phenomena were most evident in cells seeded on A8 and A15 scaffolds (Fig. 4k, l). The neurites that appeared as continuous, straight lines delineated places for cell-fiber co-localization, where aligned fibers guided neurite outgrowth of the ESC attached to the fibers and enhanced neuronal differentiation.

Combining above results, it is not sufficient to conclude any one scaffold out of the six used in this study was the absolute best at promoting neuronal differentiation. It is important that immunofluorescence experiments are repeated in the future to provide stronger evidence. Additional methods, besides Real Time PCR, that tend to be more stable can be used in future gene expression studies. Moreover, research endeavors are currently under progress to elucidate the exact cellular mechanisms behind the effects of nanofiber size and orientation of electrospun scaffolds, which will aid future investigations in their potentials for neural tissue engineering purposes.

Acknowledgements

This study was supported by Professor Peter X. Ma, Department of Biomedical Engineering, University of Michigan – Ann Arbor. This study was also supported by Rackham Graduate Student Research Grant, Rackham Graduate School, University of Michigan - Ann Arbor. Immunofluorescent experiments were done under the supervision of Mr. Jeremy Holzwarth, PhD candidate, Department of Biomedical Engineering, University of Michigan - Ann Arbor.

References

1. S.K. Bhatia. *Biotechnol J* 2010; 5:1309-1323.

2. L.G. Griffith, G. Naughton. *Science* 2002; 295:1009-1014.

3. A. Atala, F.K. Kasper, A.G. Mikos. *Sci Transl Med* 2012; 4:160rv12.

4. R. Levi-Montalcini. "Chapter 4. Conclusions and Recommendations." Neurological Disorders: Public Health Challenges. Geneva: World Health Organization. 2006; p177.

5. R.P. Lanza, R. Langer, J. Vacanti, M. Martins-Green. "Dynamics of Cell–ECM Interaction". Principles of tissue engineering. San Diego: Academic Press. 2000; p33-55.

6. E. Zamir, B. Geiger. *J Cell Sci* 2001; 114:3583-3590.

7. J.M. Holzwarth, P.X. Ma. *J Mater Chem* 2011; 21:10243-10250.

8. V.J. Chen and P.X. Ma. *Biomaterials* 2006; 27:3708-3715.

9. T. Elsdale, J. Bard. *J Cell Biol* 1972; 54:626-637.

10. J. Riesle, A.P. Hollander, R. Langer, L.E. Freed, G. Vunjak-Novakovic. *J Cell Biochem* 1998; 71:313-327.

11. P.X. Ma, R. Zhang. *J Biomed Mater Res* 1999; 46:60-72.

12. G.M. Whitesides, J.P. Mathias and C.T. Seto. *Science* 1991; 254:1312-1319.

13. D.H. Reneker, I. Chun. *Nanotechnology* 1996; 7:216-223.

14. R. Zhang, P.X. Ma. *J Biomed Mater Res* 1999; 44:446-455.

15. B. Carlberg, M.Z. Axell, U. Nannmark, J. Liu, H.G. Kuhn. *Biomed Mater* 2009; 4:045004.

16. A.S. Badami, M.R. Kreke, M.S. Thompson, J.S. Riffle, A.S. Goldstein. *Biomaterials* 2006; 27:596-606.

17. A. Berkessel, J.A. Adrio, D. Hüttenhain, J.M. Neudörfl. *J Am Chem Soc* 2006; 128:8421-8426.

18. F. Yang, R. Murugan, S. Wang, S. Ramakrishna. *Biomaterials* 2005; 26:2603-2610.

19. L. He, S. Liao, D. Quan, K. Ma, C. Chan, S. Ramakrishna, J. Lu. *Acta Biomaterialia* 2010; 6:2960-2969.

20. J.Y. Lee, C.A. Bashur, A.S. Goldstein, C.E. Schmidt. *Biomaterials* 2009; 30:4325-4335.

21. J. Xie, S.M. Willerth, X. Li, M.R. Macewan, A. Rader, S.E. Sakiyama-Elbert, Y. Xia. *Biomaterials* 2009; 30:354-362**.**

22. X. Zeng, M.S. Rao. *Neuroscience* 2007; 145:1348-1358.

23. J.W. McDonald, X.Z. Liu, Y. Qu, S. Liu, S.K. Mickey, D. Turetsky. *Nat Med* 1999; 5:1410-1412.

24. D.M. Deshpande, Y.S. Kim, T. Martinez, J. Carmen, S. Dike, I. Shats. *Ann Neurol* 2006; 60:32-44.

25. L. Cui, J. Jiang, L. Wei, X. Zhou, J.L. Fraser, B.J. Snider. *FASEB J* 2007; 21:1-11.

26. L. Cui, J. Jiang, L. Wei, X. Zhou, J.L. Fraser, B.J. Snider. *Stem Cells* 2008; 26:1356-1365.

27. H.J. Kong, J. Liu, K. Riddle, T. Matsumoto, K. Leach, D.J. Mooney. *Nat Mater* 2005; 4:460-464.

28. D.E. Ingber. *Proc Natl Acad Sci USA* 2005; 102:11571-11572.

29. A.S. Andersson, F. Backhed, A.V. Euler, A. Richter-Dahlfors, D. Sutherland, B. Kasemo. *Biomaterials* 2003; 24:3427-3436.

30. G.T. Christopherson, H.J. Song, H.Q. Mao. *Biomaterials* 2009; 30:556-564.

31. T. Liu, J.D. Houle, J. Xu, B.P. Chan, S.Y. Chew. *Tissue Eng* 2012; 18: 1057-1066.

32. A. Theron, E. Zussman, A.L. Yarin. *Nanotechnology* 2001; 12:384-390.

33. S.D. Vrieze, T.V. Camp, A. Nelvig, B. Hagström, P. Westbroek, K.D. Clerck. *J Mater Sci* 2009; 44:1357-1362.

34. G.J. Brewer. *J Neurosci Res* 1995; 42:674-683.

35. K.M. Woo, V.J. Chen, P.X. Ma. *J Biomed Mater Res* 2003; 167:531-537.

36. A.S. Badami, M.R. Kreke, M.S. Thompson, J.S. Riffle, A.S. Goldstein. *Biomaterials* 2006; 27:596-606.